Solving Darcy equation by lowest order weak Galerkin (WG) finite element method on general polygonal meshes

Zhuoran Wang

Colorado State University

Acknowledgements

Advisors

- Dr. James Liu: *ColoState*
- Dr. Simon Tavener: *ColoState*

Funding

- National Science Foundation DMS-1419077
- *ColoState* CIMS Graduate Fellowship Summer 2016

Talk Outline

- Darcy Equation
- Wachspress Coordinates
- Chen-Wang $H(\text{div})$-element CW_0
- $WG(P_0, P_0; CW_0)$ on Polygons
- WG Scheme for Darcy
- Numerical Experiments: 3 Examples
- Summary

Darcy Equation

Darcy equation usual form:

$$\begin{cases} \nabla \cdot (-\mathbf{K}\nabla p) \equiv \nabla \cdot \mathbf{u} = f, \quad \mathbf{x} \in \Omega, \\ p = p_D, \ \ \mathbf{x} \in \Gamma^D, \qquad \mathbf{u} \cdot \mathbf{n} = u_N, \ \ \mathbf{x} \in \Gamma^N, \end{cases} \tag{1}$$

- p is the unknown pressure
- $\mathbf{K}$ is a permeability tensor
- f is a source term
- p_D is Dirichlet boundary data
- u_N is Neumann boundary data

Work Have Done

Liu,Tavener,Wang, *J. Comput. Phys.* (In revision)

$\mathbf{RT_{[0]}}$:

- Basis functions are $\left\{ \begin{bmatrix} 1 \\ 0 \end{bmatrix}, \begin{bmatrix} 0 \\ 1 \end{bmatrix}, \begin{bmatrix} X \\ Y \end{bmatrix}, \begin{bmatrix} X \\ -Y \end{bmatrix} \right\}$
- Asymptotically parallelogram quadrilateral meshes

Liu,Wang *Submitted*

$\mathbf{CW_0}$:

- Basis functions rely on normalized coordinates and Wachspress coordinates
- General polygonal meshes
- Applicable to general quadrilateral meshes

Barycentric Coordinates on Triangles

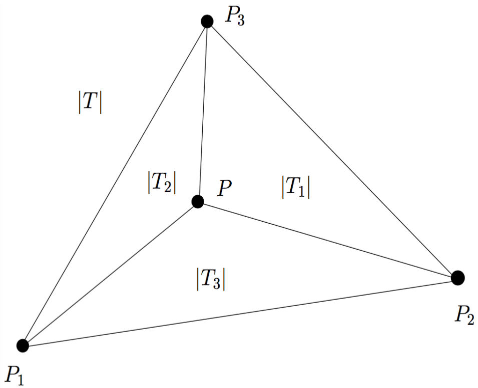

Figure: Triangle geometric information for barycentric coodinates

Wachspress Coordinates

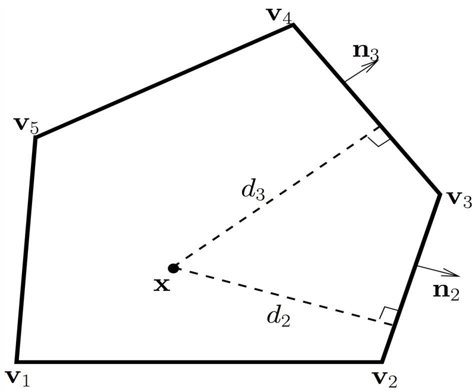

Figure: A pentagon with quantities needed for computing Wachspress coordinates

Wachspress Coordinates

Let E be a convex polygon, $\mathbf{v}_i$ are vertices, $\mathbf{n}_i$ are outward unit normal vector, $\mathbf{x} \in E^\circ$. Then its distance to edge e_i is

$$d_i = (\mathbf{v}_i - \mathbf{x}) \cdot \mathbf{n}_i, \quad 1 \leq i \leq n. \tag{2}$$

A scaled normal vector is

$$\tilde{\mathbf{n}}_i = \frac{1}{d_i}\mathbf{n}_i, \quad 1 \leq i \leq n. \tag{3}$$

And

$$w_i(\mathbf{x}) = \det(\tilde{\mathbf{n}}_i, \tilde{\mathbf{n}}_{i+1}), \quad W(\mathbf{x}) = \sum_{i=1}^{n} w_i(\mathbf{x}). \tag{4}$$

Then the **Wachspress coordinates** are

$$\lambda_i(\mathbf{x}) = w_i(\mathbf{x})/W(\mathbf{x}), \quad 1 \leq i \leq n. \tag{5}$$

Wachspress Coordinates: Gradients, Curls

Wachspress coordinates are rational functions. They satisfy:

$$\lambda_i(\mathbf{x}) \geq 0, \quad \sum_{i=1}^{n} \lambda_i(\mathbf{x}) = 1, \quad \sum_{i=1}^{n} \lambda_i(\mathbf{x})\mathbf{v}_i = \mathbf{x},$$

Gradients of Wachspress coordinates:

$$\nabla \lambda_i(\mathbf{x}) = \lambda_i(\mathbf{x})(\mathbf{R}_i - \sum_{j=1}^{n} \lambda_j \mathbf{R}_j), \quad 1 \leq i \leq n, \tag{6}$$

where $\mathbf{R}_i(\mathbf{x}) = \frac{\nabla w_i(\mathbf{x})}{w_i(\mathbf{x})}$.

Curls of Wachspress coordinates:

$$\mathrm{curl}(\lambda_i) = \begin{bmatrix} -\partial_y \lambda_i \\ \partial_x \lambda_i \end{bmatrix} = \begin{bmatrix} 0 & -1 \\ 1 & 0 \end{bmatrix} \nabla \lambda_i, \quad 1 \leq i \leq n. \tag{7}$$

Wachspress Coordinates on Special Quadrilateral

E is a quadrilateral with vertices $(0,0)$, $(1,0)$, (a,b), $(0,1)$. The Wachspress coordinates are

$$\lambda_i(x,y) = f_i(x,y)/g(x,y), \qquad i = 1,2,3,4, \tag{8}$$

where

$$\begin{cases} g(x,y) = ab + b(b-1)x + a(a-1)y, \\ f_1(x,y) = ab + (b(b-1)-ab)x + (a(a-1)-ab)y \\ \qquad\qquad -b(b-1)x^2 + (2ab-a-b+1)xy - a(a-1)y^2, \\ f_2(x,y) = abx + b(b-1)x^2 - abxy, \\ f_3(x,y) = (a+b-1)xy, \\ f_4(x,y) = aby - abxy + a(a-1)y^2. \end{cases}$$

Wachspress Coordinates on Special Quadrilateral

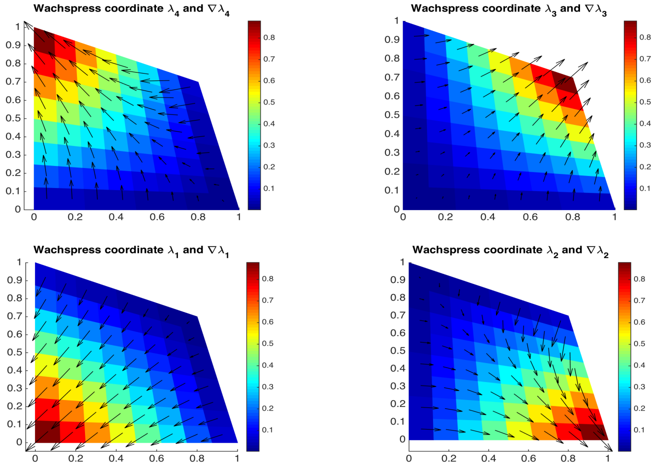

Figure: The Wachspress coordinate functions and their gradients on a quadrilateral with vertices located at $(0, 0)$, $(1, 0)$, $(0.8, 0.7)$, and $(0, 1)$.

Chen-Wang $H(\text{div})$-element CW_0

Chen,Wang, *Math. Comput.* (2017)
Basis function of CW_0 element is

$$\mathbf{w}_i = a_i(\mathbf{x} - \mathbf{x}_c) + \sum_{j=1}^{n} c_{i,j}\text{curl}(\lambda_j), \quad 1 \le i \le n, \tag{9}$$

where λ_j are Wachspress coordinates, $a_i, b_{i,j}, c_{i,j}$ are coeficients,

- $a_i = |e_i|/(2|E|)$,
- $b_{i,j} = \delta_{i,j}|e_j| - |e_j||T_j|/|E|$,
- $c_{i,j} = -\frac{1}{n}\sum_{k=1}^{n-1} kb_{i,j+k}, \quad 1 \le i,j \le n$,

$\mathbf{v}_i$ are vertices, $\mathbf{x}_c = (x_c, y_c)$ is the geometric center of E, $|E|$ is the area, $|T_i|$ is the area of the triangle formed by $\mathbf{x}_c, \mathbf{v}_i, \mathbf{v}_{i+1}$.

Basis for CW_0 Element

Properties

- $\mathbf{w}_i|_{e_j} \cdot \mathbf{n}_j = \delta_{i,j}$
- $\nabla \cdot \mathbf{w}_i = 2a_i, \quad \forall 1 \leq i, j \leq n$

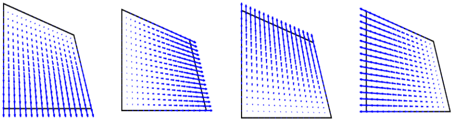

Figure: Four basis functions for CW_0 on a quadrilateral with vertices $(0,0), (1,0), (0.8, 0.7), (0, 1)$.

WG(P_0, P_0; CW_0) on Polygons

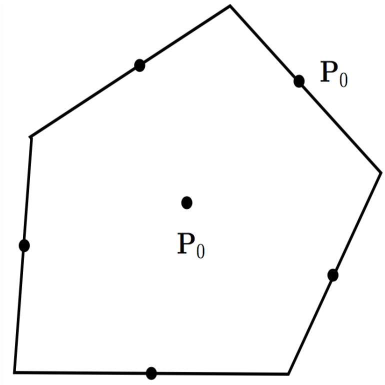

Figure: $WG(P_0, P_0)$ basis functions inside and on the edges of a pentagon.

Discrete Weak Gradients

Discrete weak function has 2 independent pieces:

$$\phi = \{\phi^\circ, \phi^\partial\}, \phi^\circ \in P^0(E^\circ), \phi^\partial \in P^0(E^\partial).$$

Discrete weak gradients are specified in certain spaces via integration by parts.

Discrete weak gradient $\nabla_{w,d}\phi \in CW_0$, is the unique solution of

$$\int_E (\nabla_{w,d}\phi) \cdot \mathbf{w} = \int_{E^\partial} \phi^\partial (\mathbf{w} \cdot \mathbf{n}) - \int_{E^\circ} \phi^\circ (\nabla \cdot \mathbf{w}), \quad \mathbf{w} \in CW_0,$$

solving a small size SPD linear system.

Discrete Weak Gradients

For example, on a quadrilateral element E, the right hand sides of 5 basis functions are

$$\begin{bmatrix} -|e_1| \\ -|e_2| \\ -|e_3| \\ -|e_4| \end{bmatrix}, \quad \begin{bmatrix} |e_1| \\ 0 \\ 0 \\ 0 \end{bmatrix}, \quad \begin{bmatrix} 0 \\ |e_2| \\ 0 \\ 0 \end{bmatrix}, \quad \begin{bmatrix} 0 \\ 0 \\ |e_3| \\ 0 \end{bmatrix}, \quad \begin{bmatrix} 0 \\ 0 \\ 0 \\ |e_4| \end{bmatrix}.$$

WG Scheme for Pressure

Seek $p_h = \{p_h^\circ, p_h^\partial\} \in S_h$ such that $p_h^\partial|_{\Gamma_h^D} = Q_h^\partial(p_D)$ (L^2-projection of Dirichlet boundary data into the space of piecewise constants on Γ_h^D) and

$$\mathcal{A}_h(p_h, q) = \mathcal{F}(q), \qquad \forall q = \{q^\circ, q^\partial\} \in S_h^0, \tag{10}$$

where

$$\mathcal{A}_h(p_h, q) := \sum_{E \in \mathcal{E}_h} \int_E \mathbf{K} \nabla_{w,d} p_h \cdot \nabla_{w,d} q, \tag{11}$$

and

$$\mathcal{F}(q) := \sum_{E \in \mathcal{E}_h} \int_E f\, q^\circ - \sum_{\gamma \in \Gamma_h^N} \int_\gamma u_N q^\partial. \tag{12}$$

WG for Darcy on a Polygonal Mesh: Velocity, Normal Flux

Numerical Velocity:

$$\mathbf{u}_h = \mathbf{Q}_h(-\mathbf{K}\nabla_{w,d}p_h),$$

when $\mathbf{K}$ is a scalar matrix, this projection is not needed.

Bulk normal flux on an edge:

$$\int_{e\in E^\partial} \mathbf{u}_h \cdot \mathbf{n}_e.$$

Properties of the Lowest-order WG Scheme

Theorem 1: Local mass conservation

$$\int_E f = \int_{E^\partial} \mathbf{u}_h \cdot \mathbf{n}.$$

Proof. Take a test function q so that $q|_{E^\circ} = 1$ but vanishes on all edges and inside all other elements. Then

$$\begin{aligned}\int_E f &= \int_E (\mathbf{K}\nabla_{w,d} p_h) \cdot \nabla_{w,d} q = \int_E R_h(\mathbf{K}\nabla_{w,d} p_h) \cdot \nabla_{w,d} q \\ &= -\int_E \mathbf{u}_h \cdot \nabla_{w,d} q = -\int_{E^\partial} q^\partial (\mathbf{u}_h \cdot \mathbf{n}) + \int_{E^\circ} q^\circ (\nabla \cdot \mathbf{u}_h) \\ &= \int_{E^\circ} \nabla \cdot \mathbf{u}_h = \int_{E^\partial} \mathbf{u}_h \cdot \mathbf{n}.\end{aligned}$$

Theorem 2: Continuity of bulk normal fluxes

If $\partial E_1 \cap \partial E_2 = \gamma$, $\mathbf{n_1}, \mathbf{n_2}$ are the constant outward unit normal vectors on γ, there holds

$$\int_\gamma \mathbf{u}_h^{(1)} \cdot \mathbf{n}_1 + \int_\gamma \mathbf{u}_h^{(2)} \cdot \mathbf{n}_2 = 0.$$

Proof. We take a test function $q = \{q^\circ, q^\partial\}$ such that $q^\partial = 1$ only on the very edge γ; but $q^\partial = 0$ on all other edges and $q^\circ = 0$ in interior of any quadrilateral or triangular element. We have

$$\begin{aligned}
0 &= \int_{E_1} (\mathbf{K}\nabla_{w,d} p_h) \cdot \nabla_{w,d} q + \int_{E_2} (\mathbf{K}\nabla_{w,d} p_h) \cdot \nabla_{w,d} q \\
&= \int_{E_1} R_h(\mathbf{K}\nabla_{w,d} p_h) \cdot \nabla_{w,d} q + \int_{E_2} R_h(\mathbf{K}\nabla_{w,d} p_h) \cdot \nabla_{w,d} q \\
&= \int_{E_1} (-\mathbf{u}_h^{(1)}) \cdot \nabla_{w,d} q + \int_{E_1} (-\mathbf{u}_h^{(2)}) \cdot \nabla_{w,d} q \\
&= -\int_\gamma \mathbf{u}_h^{(1)} \cdot \mathbf{n}_1 - \int_\gamma \mathbf{u}_h^{(2)} \cdot \mathbf{n}_2.
\end{aligned}$$

Convergence in Pressure, Velocity and Flux

L^2-norms:

$$\|p - p_h^\circ\|^2 = \sum_{E \in \mathcal{E}_h} \|p - p_h^\circ\|_{L^2(E)}^2, \tag{13}$$

$$\|\mathbf{u} - \mathbf{u}_h\|^2 = \sum_{E \in \mathcal{E}_h} \|\mathbf{u} - \mathbf{u}_h\|_{L^2(E)^2}^2, \tag{14}$$

$$\|(\mathbf{u} - \mathbf{u}_h) \cdot \mathbf{n}\|^2 = \sum_{E \in \mathcal{E}_h} \sum_{\gamma \subset E^\partial} \frac{|E|}{|\gamma|} \|\mathbf{u} \cdot \mathbf{n} - \mathbf{u}_h \cdot \mathbf{n}\|_{L^2(\gamma)}^2. \tag{15}$$

Theorem 3: Assume $p \in H^2(\Omega), \mathbf{u} \in H^1(\Omega)$, $\mathbf{u}_h$ is the numerical velocity, then

$$\|\mathbf{u} - \mathbf{u}_h\| \lesssim h. \tag{16}$$

Theorem 4: Assume $p \in H^2(\Omega), \mathbf{u} \in H^1(\Omega)$, $\mathbf{u}_h$ is the numerical velocity, then

$$\|\mathbf{u} \cdot \mathbf{n} - \mathbf{u}_h \cdot \mathbf{n}\| \lesssim h. \tag{17}$$

Theorem 5: Assume $p \in H^2(\Omega), \mathbf{u} \in H^1(\Omega)$, then

$$\|p - p_h^\circ\| \lesssim h. \tag{18}$$

Comparing with Continuous Galerkin Method

In CG method, Wachspress coordinates are used as basis functions.

Advantage: Has the least degrees of freedom.

Disadvantage: Doesn't satisfy local mass conservation or normal flux continuity.

Numerical Experiments: 3 Types of Meshes

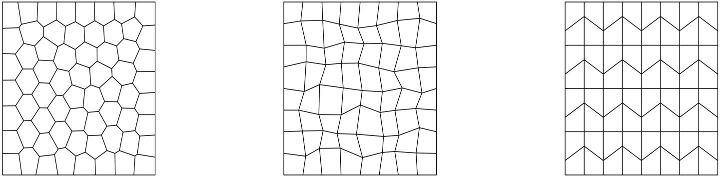

Figure: Types of meshes: Left: A polygonal mesh generated by *PolyMesher*; Middle: A randomly h-perturbed quadrilateral mesh; Right: A trapezoidal mesh.

Mu,Wang,Ye,*IJNAM* (2015)
The exact solution is $p(x,y) = x(1-x)y(1-y)$ with homogeneous Dirichlet boundary condition defined on the bottom, top and left, Neumann boundary condition is on the right, $\Omega = (0,1)^2$, $\mathbf{K} = xy\mathbf{I}_2$. We can calculate that

$$\mathbf{u} = [-x(1-2x)y^2(1-y), -x^2(1-x)y(1-2y)],$$

and

$$f = -(1-4x)y^2(1-y) - x^2(1-x)(1-4y).$$

Numerical Experiments: Example 1

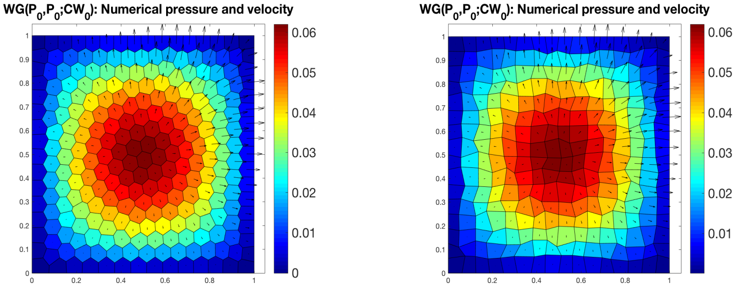

Figure: $WG(P_0, P_0; CW_0)$ numerical pressure and velocity with $h = \frac{1}{16}$.

Numerical Experiments: Example 1

Liu,Wang *Submitted*

Table: Example 1: Results of WG($P_0, P_0; CW_0$) on polygonal meshes generated by `PolyMesher`

#Elem	h	$\|p - p_h^\circ\|$	rate	$\|\mathbf{u} - \mathbf{u}_h\|$	rate	$\|(\mathbf{u} - \mathbf{u}_h) \cdot \mathbf{n}\|$	rate
$(2^3)^2$	1.89E-1	5.780E-3	–	5.651E-3	–	9.177E-3	–
$(2^4)^2$	9.23E-2	2.700E-3	1.09	2.394E-3	1.23	4.221E-3	1.12
$(2^5)^2$	4.57E-2	1.335E-3	1.01	1.004E-3	1.25	1.879E-3	1.16
$(2^6)^2$	2.28E-2	6.684E-4	0.99	4.661E-4	1.10	8.709E-4	1.10

Table: Example 1: Results of WG($P_0, P_0; CW_0$) on randomly h-perturbed quadrilateral meshes

$1/h$	$\|p - p_h^\circ\|$	$\|\mathbf{u} - \mathbf{u}_h\|$	$\|(\mathbf{u} - \mathbf{u}_h) \cdot \mathbf{n}\|$
2^3	5.7065e-03	6.8578e-03	9.9357e-03
2^4	2.8499e-03	3.6151e-03	5.0437e-03
2^5	1.4276e-03	1.8198e-03	2.4787e-03
2^6	7.0955e-04	9.2219e-04	1.2450e-03
2^7	3.5357e-04	4.6155e-04	6.2157e-04
Rate	1st order	1st order	1st order

Numerical Experiments: Example 2

The exact solution is $p(x, y) = \sin(\pi x)\sin(\pi y)$ with homogeneous Dirichlet boundary condition on the whole boundary, $\Omega = (0, 1)^2$, $\mathbf{K} = \mathbf{I}_2$.

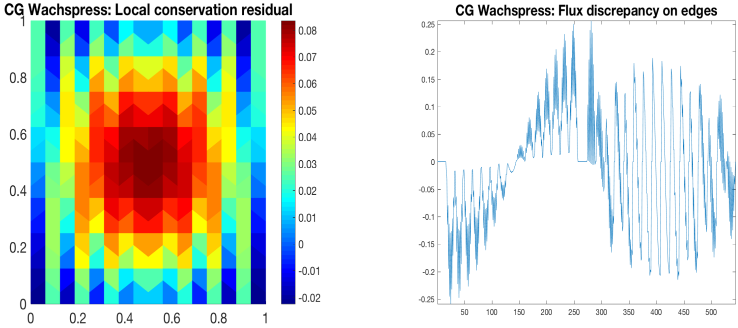

Figure: Continuous Galerkin FEM with Wachspress coordinates, $h = \frac{1}{16}$.

Numerical Experiments: Example 2

Liu,Wang,*Submitted*

Table: Example 2: Results of three numerical methods on trapezoidal meshes

	WG($P_0, P_0; CW_0$)		WG($P_1, P_0; P_0^2$) penalty $\rho = 1$	CG Wachspress	
$1/h$	$\|p - p_h^\circ\|$	$\|\mathbf{u} - \mathbf{u}_h\|$	$\|p - p_h^\circ\|$	$\|p - p_h\|$	$\|\mathbf{u} - \mathbf{u}_h\|$
8	8.339E-2	2.743E-1	6.616E-2	1.271E-2	3.202E-1
16	4.181E-2	1.385E-1	1.667E-2	3.227E-3	1.610E-1
32	2.092E-2	6.971E-2	4.183E-3	8.098E-4	8.066E-2
64	1.046E-2	3.497E-2	1.047E-3	2.026E-4	4.035E-2
128	5.231E-3	1.752E-2	2.620E-4	5.067E-5	2.017E-2
Rate	1st order	1st order	2nd order	2nd order	1st order

Numerical Experiments: Example 3

Arnold,Boffi,Falk,*MCOM* (2002) p. 918.
Liu,Wang *Submitted*

The exact solution is $p(x, y) = x^3 + 5y^2 - 10y^3 + y^4$ with homogeneous Dirichlet boundary condition on the whole boundary, $\Omega = (0, 1)^2$, $\mathbf{K} = \mathbf{I}_2$. We can calculate that

$$f = -(6x + 10 - 60y + 12y^2).$$

Table: Example 3: Superconvergence of $\|p_h^\circ - Q_h^\circ p\|$ and 1st order convergence in div on randomly h-perturbed quadrilateral meshes

h	$\|p_h^\circ - Q_h^\circ p\|$	Rate	$\mathrm{div}(\mathbf{u} - \mathbf{u}_h)$	Rate
$1/2^3$	2.3515e-03	–	1.8171e-0	–
$1/2^4$	6.4020e-04	1.87	9.1842e-01	0.98
$1/2^5$	1.6776e-04	1.93	4.6157e-01	0.99
$1/2^6$	4.4475e-05	1.91	2.3061e-01	1.00
$1/2^7$	1.1364e-05	1.96	1.1527e-01	1.00

Nice Features

The advantages:

- Applicable to convex polygons
- SPD linear system
- No need for penalization
- Constants approximants
- Local mass conservation and flux continuity
- Optimal order convergence in pressure, velocity and flux

D. Arnold, D. Boffi, and R. Falk.
Approximation by quadrilateral finite elements.
Math. Comput., 71:909–922, 2002.

J. Liu and Z. Wang.
Lowest-order weak galerkin finite element method for darcy flow on general polygonal meshes.
Submitted.

L. Mu, J. Wang, and X. Ye.
Weak galerkin finite element methdos on polytopal meshes.
Int. J. Numer. Anal. Model., 12:31–53, 2015.